Different cardiovascular and pulmonary phenotypes for single- and double-knock-out mice deficient in BMP9 and BMP10

Claire Bouvard, Ly Tu, Martina Rossi, Agnès Desroches-Castan, Nihel Berrebeh, Elise Helfer, Caroline Roelants, Hequn Liu, Marie Ouarne, Nicolas Chaumontel, et al.

Cardiovascular Research
doi:10.1093/cvr/cvab187

Different cardiovascular and pulmonary phenotypes for single- and double-knock-out mice deficient in BMP9 and BMP10

Claire Bouvard [1*], Ly Tu [2,3], Martina Rossi[1], Agnès Desroches-Castan [1], Nihel Berrebeh [2,3], Elise Helfer [1], Caroline Roelants[1,4], Hequn Liu [1], Marie Ouarné[1†], Nicolas Chaumontel[1], Christine Mallet[1], Christophe Battail [1], Andreas Bikfalvi [5], Marc Humbert [2,3,6], Laurent Savale[2,3,6], Thomas Daubon[5,7], Pascale Perret [8], Emmanuelle Tillet[1], Christophe Guignabert [2,3‡], and Sabine Bailly [1‡]

[1]Laboratoire Biosanté U1292, Université Grenoble Alpes, INSERM, CEA, IRIG-Biosanté UMR_S 1292, 38000 Grenoble, France; [2]School of Medicine, Université Paris-Saclay, Le Kremlin-Bicêtre, France; [3]INSERM UMR_S 999, Hôpital Marie Lannelongue, Le Plessis-Robinson, France; [4]Inovarion, 75005 Paris, France; [5]INSERM U1029, Institut National de la Santé et de la Recherche Médicale, 33615 Pessac, France; [6]AP-HP, Department of Respiratory and Intensive Care Medicine, Hôpital Bicêtre, Le Kremlin-Bicêtre, France; [7]Univ. Bordeaux, CNRS, IBGC, UMR5095, 33000 Bordeaux, France; and [8]Laboratory of Bioclinical Radiopharmaceutics, Université Grenoble Alpes, INSERM, UMRS_1039, LRB, 38000 Grenoble, France

Received 1 October 2020; editorial decision 23 May 2021

Aims *BMP9* and *BMP10* mutations were recently identified in patients with pulmonary arterial hypertension, but their specific roles in the pathogenesis of the disease are still unclear. We aimed to study the roles of BMP9 and BMP10 in cardiovascular homeostasis and pulmonary hypertension using transgenic mouse models deficient in *Bmp9* and/or *Bmp10*.

Methods and results Single- and double-knockout mice for *Bmp9* (constitutive) and/or *Bmp10* (tamoxifen inducible) were generated. Single-knock-out (KO) mice developed no obvious age-dependent phenotype when compared with their wild-type littermates. However, combined deficiency in *Bmp9* and *Bmp10* led to vascular defects resulting in a decrease in peripheral vascular resistance and blood pressure and the progressive development of high-output heart failure and pulmonary hemosiderosis. RNAseq analysis of the lungs of the double-KO mice revealed differential expression of genes involved in inflammation and vascular homeostasis. We next challenged these mice to chronic hypoxia. After 3 weeks of hypoxic exposure, *Bmp10*-cKO mice showed an enlarged heart. However, although genetic deletion of *Bmp9* in the single- and double-KO mice attenuated the muscularization of pulmonary arterioles induced by chronic hypoxia, we observed no differences in *Bmp10*-cKO mice. Consistent with these results, endothelin-1 levels were significantly reduced in *Bmp9* deficient mice but not *Bmp10*-cKO mice. Furthermore, the effects of BMP9 on vasoconstriction were inhibited by bosentan, an endothelin receptor antagonist, in a chick chorioallantoic membrane assay.

Conclusions Our data show redundant roles for BMP9 and BMP10 in cardiovascular homeostasis under normoxic conditions (only combined deletion of both *Bmp9* and *Bmp10* was associated with severe defects) but highlight specific roles under chronic hypoxic conditions. We obtained evidence that BMP9 contributes to chronic hypoxia-induced pulmonary vascular remodelling, whereas BMP10 plays a role in hypoxia-induced cardiac remodelling in mice.

* Corresponding author. Tel: +33 4 38 78 42 25; fax: +33 4 38 78 50 58, E-mail: claire.bouvard@univ-grenoble-alpes.fr
† Present address. Instituto de Medicina Molecular, Faculdade de Medicina, Universidade de Lisboa, Lisbon, Portugal.
‡ The last two authors contributed equally to this work.

Graphical Abstract

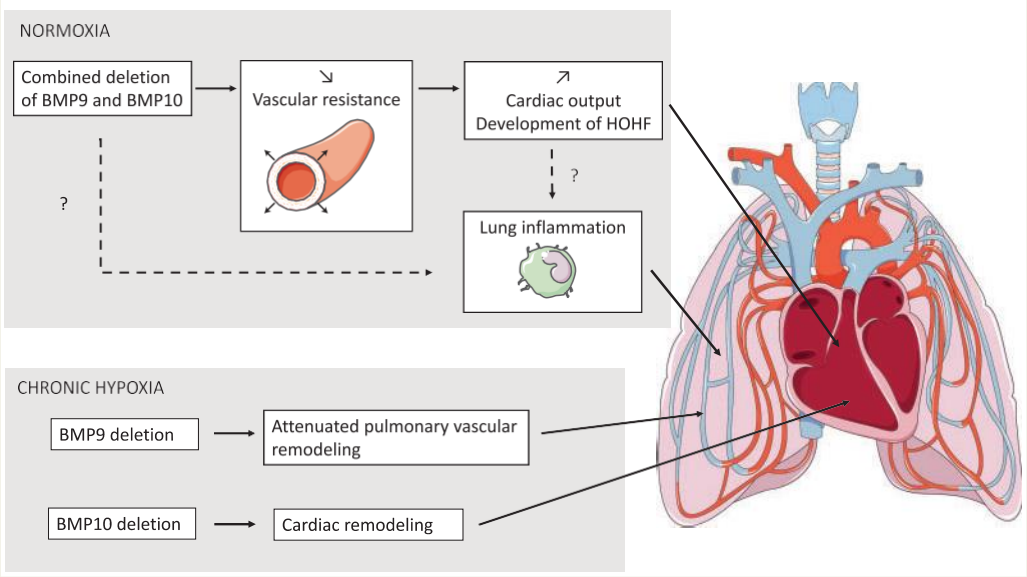

Keywords Pulmonary hypertension • Pulmonary vascular remodelling • Vascular anomalies • High-output heart failure • Bone morphogenetic proteins

1. Introduction

Pulmonary arterial hypertension (PAH) refers to an incurable rare and lethal cardiopulmonary disorder that affects both the structure and function of blood vessels of the heart and lungs.[1,2] Although the aetiology and underlying mechanisms are still unknown, many PAH-predisposing factors have been recently identified, including mutations in the genes encoding BMPRII and ALK1 (*BMPR2* and *ACVRL1*, respectively)[3,4] and, more recently, in those encoding one of the major ligands of BMPRII/ALK1 heterocomplexes, namely BMP9 and BMP10 (*BMP9*, also named *GDF2*, and *BMP10*, respectively).[5–9] Consequently, the loss or dysfunction of BMPRII/ALK1 signalling are currently considered to be the major molecular defects responsible for the predisposition to PAH and disease progression. Heterozygous mutations in the *ACVRL1* and *ENG* genes and, less frequently, *BMP9* mutations have also been shown to be associated with hereditary haemorrhagic telangiectasia (HHT), another rare disease, characterized by various vascular defects, including epistaxis, blood vessel dilation (telangiectasia), and arteriovenous malformations (AVMs) in several organs.[10–12] The mechanism by which defects in this signalling pathway predispose individuals to HHT and/or PAH and alters cardiovascular function and pulmonary blood flow is still unknown.

BMP9 and BMP10 share a high degree of sequence identity (64% in the mature domain) and have been found to have both redundant and specific roles due to their expression profiles and receptor affinities.[13] BMP9 is mainly produced by hepatic stellate cells (HSCs),[14,15] whereas BMP10 is produced mainly by the heart[16–18] and only at low levels by HSCs.[15] They are both present in the circulating blood[18–20] and were shown to bind to the endothelial-specific receptor ALK1 with subnanomolar affinities,[21,22] supporting a critical role for BMP9 and BMP10 in vascular remodelling. However, their binding affinities for type 2 receptors differ,[21] suggesting that they could also play specific roles. Consistent with this notion, gene deletion studies have shown that C57BL/6 mice lacking *Bmp9* are viable and fertile, with no overt defect in cardiac or blood vessel development,[23] whereas *Bmp10* knock-out (KO) mice die during embryonic development due to defective cardiac development[24] and show vascular defects.[20] The analysis of $Bmp10^{9/9}$ knock-in mice, for which the coding sequence of *Bmp10* was replaced by that of *Bmp9*, showed that although BMP9 and BMP10 appear to play redundant roles in early embryonic vascular development, BMP10 has an exclusive function in embryonic cardiac development that cannot be replaced by BMP9.[20] We have also demonstrated that BMP9 and BMP10 exhibit redundant roles in postnatal retinal vascularization and ductus arteriosus closure.[23,25] In our previous study, we unexpectedly showed that genetic deletion or inhibition of BMP9 (using an inhibitory antibody or the soluble ALK1 receptor as a ligand trap) had beneficial effects against the onset and progression of pulmonary hypertension (PH) in several experimental animal models.[26] These results appear to contradict those published by another group that demonstrated the capacity of recombinant BMP9 to attenuate PH in animal models.[27,28] Overall, these findings suggest that BMP9 and BMP10 may play a role in cardiovascular homeostasis and are involved in the development of PAH, but that further work is necessary to understand their respective roles. Although the phenotype of adult *Bmp9* knockout mice has been previously described,[26] the long-term effects of the loss of *Bmp10* or that of both *Bmp9* and *Bmp10* in adult mice have never been thoroughly studied.

We aimed to investigate and compare the roles of BMP9 and BMP10 in cardiovascular homeostasis and PH using adult single-KO and double-KO mice for *Bmp9* (constitutive deletion) and/or *Bmp10* (tamoxifen-induced deletion to bypass embryonic lethality) under both normoxic and hypoxic conditions to induce PH.

2. Methods

Methods are detailed in the Supplementary material online.

2.1 *Bmp9*-KO, *Bmp10*-cKO, and DKO mouse models

We generated C57BL/6 mice lacking *Bmp10* and/or *Bmp9* as previously described.[23,29] Briefly, constitutive deletion of *Bmp9* resulted from the replacement of exon 2 by a neomycin-resistance cassette. Because *Bmp10* deletion leads to early embryonic lethality, we used the tamoxifen-inducible Cre system to generate *Bmp10*-cKO mice (Rosa26-CreER^{T2}; *Bmp10*$^{lox/lox}$) by crossing Rosa26-CreER^{T2} mice (generously provided by Pr P. Chambon, IGBMC, Illkirch, France) with *Bmp10*$^{lox/lox}$ mice, which possess loxP sites flanking exon 2. We generated double-KO (DKO) mice by crossing the Rosa26-CreER^{T2}; *Bmp10*$^{lox/lox}$ mice with *Bmp9*-KO mice. All mice were viable. The offspring genotypes were determined by PCR as previously reported.[29]

All mice (3–4 weeks old for the PH experiments and 8 weeks old for all other experiments) were treated with tamoxifen (Sigma) by intraperitoneal injection once a day for five days at a dose of 50 mg/kg to induce Cre recombination in the *Bmp10*-cKO and DKO transgenic mice or to serve as controls. Mice were housed in a pathogen-free barrier facility under a 14-h light/10-h dark cycle and temperature-controlled environment with standard diet and water ad libitum.

2.2 Ethical approval and methods for anaesthesia and euthanasia

All animal procedures were designed to conform to the guidelines of Directive 2010/63/EU of the European Parliament on the protection of animals used for scientific purposes and the protocols used were approved by institutional ethics committees (APAFIS#17604-2018092716378446 v4; APAFIS #18715-201901301823452 v2). Gaseous anaesthesia (isoflurane 4% for induction and 1.5–2.5% for maintenance) was used for echocardiography, right heart catheterization, and fluorescent microsphere injections. Euthanasia was performed using pentobarbital injection (180 mg/kg) or by exsanguination under isoflurane.

2.3 Statistical analysis

The data are expressed as the means ± standard error of the mean (SEM). Mann–Whitney tests were used to assess the statistical significance of differences between two groups. Comparisons concerning more than two groups were calculated by analysis of variance followed by the Tukey test for data with a normal distribution or the Kruskal–Wallis and Dunn tests for data with a non-normal distribution. Differences were considered significant for $P < 0.05$. Analyses were performed using PRISM software (GraphPad).

3. Results

3.1 Phenotypic and molecular characterization of single-(KO) and DKO mice

We first studied adult single-KO and DKO mice for *Bmp9* and *Bmp10* under unstressed conditions to decipher the role of BMP9 and BMP10 in cardiovascular homeostasis. The deficiency in BMP9 and/or BMP10 was previously demonstrated[15,29] and verified here by measuring plasma concentrations of BMP9, BMP10, and BMP9-BMP10 heterodimers by ELISA (Supplementary material online, *Figure S1a*) and *Bmp9* and *Bmp10* mRNA levels in the liver (Supplementary material online, *Figure S1b*), right atria (Supplementary material online, *Figure S1c*), and lungs (Supplementary material online, *Figure S1d*). As expected, *Bmp9* was mainly expressed in the liver and *Bmp10* in the right atria and at a lower levels in the liver. *Bmp9* transcripts were absent from the *Bmp9*-KO and DKO mice and *Bmp10* mRNA levels were down-regulated in the *Bmp10*-cKO and DKO mice. We observed no compensatory changes between *Bmp9* and *Bmp10* expression (Supplementary material online, *Figure S1b–d*). Notably, circulating levels of BMP9 in *Bmp10*-cKO and BMP10 in *Bmp9*-KO mice were reduced but this might be due to the fact that the BMP9 and BMP10 ELISAs also detected the BMP9-10 heterodimeric form, as previously demonstrated [15] (Supplementary material online, *Figure S1a*).

Adult *Bmp9*-KO, *Bmp10*-cKO, and DKO mice were viable, and their body weight was not significantly different from that of wild-type (WT) mice (Supplementary material online, *Figure S2a* and *b*). Upon dissection, the single KO mice appeared to be normal, whereas the hearts and spleens of the DKO mice were significantly larger than those of all the other groups (*Figure 1A–F*, Supplementary material online, *Figure S2*). The greater size of the DKO hearts resulted from an increase in the size of both the right and left ventricles (*Figure 1E and F*, Supplementary material online, *Figure S3a* and *b*). Analysis of spleen sections stained with H&E did not reveal any obvious structural differences (Supplementary material online, *Figure S3c*). In contrast to the other groups of mice, DKO mouse lungs appeared strikingly reddish and/or brownish (although a few brown spots were occasionally noticed on single-KO lungs) (*Figure 1G*) and Prussian blue staining revealed the presence of iron-laden macrophages in DKO lungs (*Figure 1H*). We previously observed liver defects in another mouse model lacking *Bmp9* (in the 129Ola genetic background).[30] Thus, we examined this organ more closely. The colour and general aspect of the liver in the various groups appeared normal upon dissection. Picrosirius red staining showed a slight but significant increase in liver perivascular fibrosis in the *Bmp10*-cKO and DKO mice (Supplementary material online, *Figure S3d* and *e*), but hyaluronic acid (HA), ALT, and AST plasma levels were normal for all mice (Supplementary material online, *Figure S3f*, *Table S1*). We analysed standard serum chemistry and haematology parameters but observed no significant differences relative to WT mice (Supplementary material online, *Tables S1* and *S2*). Of note, the phenotype of DKO mice was similar for male and female C57BL/6 mice (Supplementary material online, *Figure S2*).

To better characterize the mice at the molecular level, we assessed mRNA levels of the main BMP9/10 receptors, *Acvrl1* (encoding the receptor ALK1), *Eng* (encoding the co-receptor endoglin), and *Bmpr2*, as well as the two BMP target genes, *Id1* [encoding the protein ID1

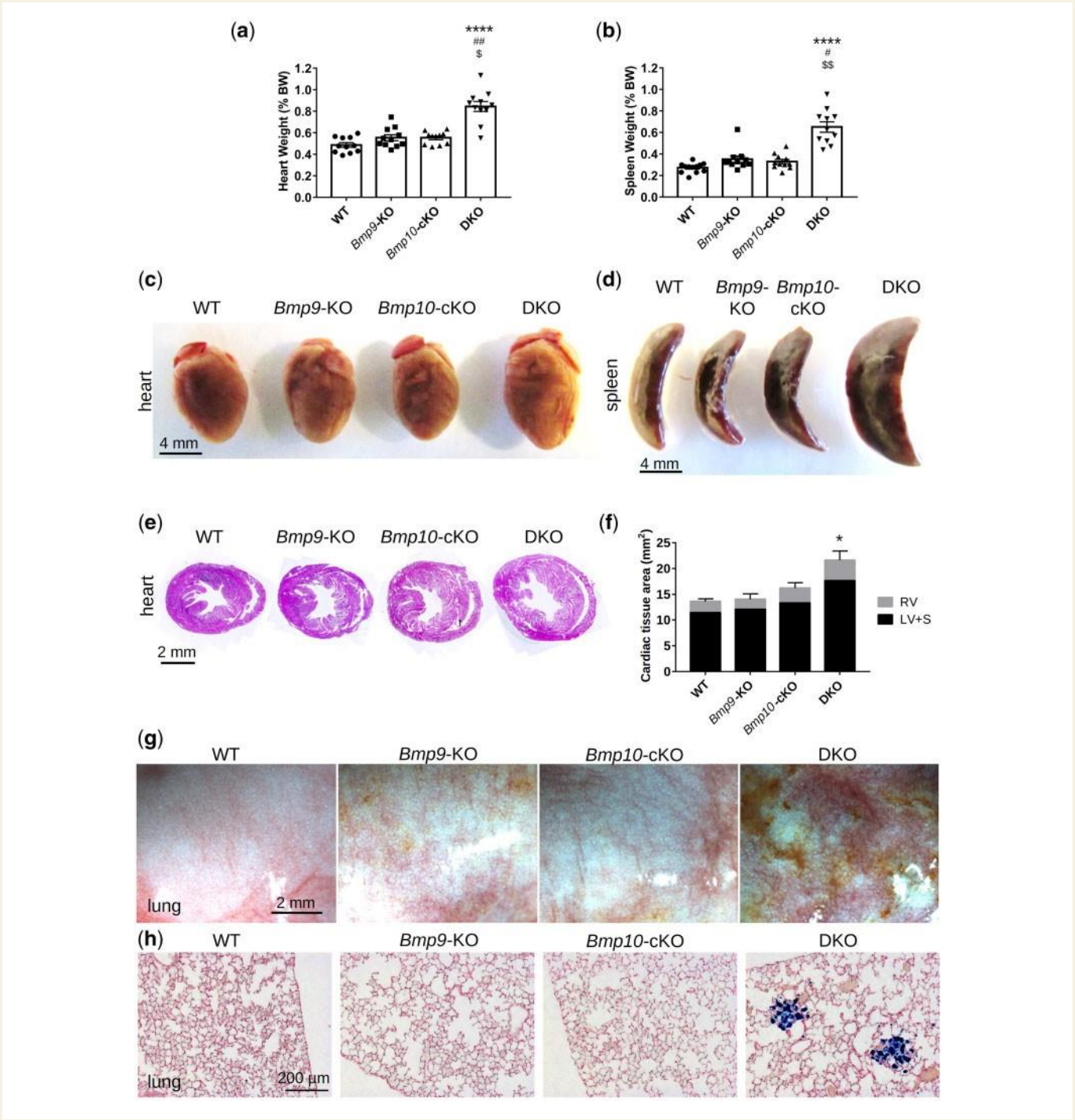

Figure 1 Combined loss of *Bmp9* and *Bmp10* leads to cardiomegaly, splenomegaly, and pulmonary hemosiderosis in DKO mice. Heart weight (*A*) and spleen weight (*B*) normalized to body weight and representative photographs of hearts (*C*) and spleens (*D*) (n = 11–12/group, male mice, scale bar = 4 mm). Representative photomicrographs of H&E-stained transverse heart sections (*E*) and quantitative analysis of the left ventricle þ septum (LVþS), right ventricle (RV), and total cardiac tissue area (*F*) (n = 4/group, female mice, scale bar = 2 mm). Representative photomicrographs of fresh lungs (scale bar = 2 mm) (*G*) and lung sections stained with Prussian blue (scale bar = 200 mM) (*H*). All mice were injected with tamoxifen at the age of 2 months and euthanized at the age of 5 months. Data are presented as the means ± SEM and were analysed using Kruskal–Wallis tests followed by Dunn's tests. $^{*}P < 0.05$, $^{****}P < 0.0001$ vs. WT; $^{\#}P < 0.05$, $^{\#\#}P < 0.01$ vs. *Bmp9*-KO; $^{\$}P < 0.05$, $^{\$\$}P < 0.01$ vs. *Bmp10*-cKO.

(inhibitor of DNA binding 1)] and *Smad6* (encoding the inhibitory protein Smad6) in lung, liver, and heart (right atria and left ventricle) tissue. We observed no significant differences between KO and WT mice, except for *Eng* (also a target gene in the BMP9/10 pathway) and *Smad6*, which were significantly down-regulated in the left ventricle and lungs of DKO mice, respectively (Supplementary material online, *Figure S4a–d*). We also analysed the BMP9/10 signalling pathways in the KO mice by western blotting. pSmad1/5/8 and pSmad2/3 protein levels were

significantly down-regulated in the lungs of *Bmp9*-KO and DKO mice but the difference vs. WT mice did not reach statistical significance in *Bmp10*-cKO mice (Supplementary material online, *Figure S4f*). There were no differences in heart tissue (data not shown).

3.2 DKO mice present signs of dilated cardiomyopathy with high output that progressively leads to heart failure

We next performed echocardiographic and cardiac histological examinations to further characterize the observed cardiac phenotype when *Bmp9* and *Bmp10* were deleted. Doppler-echocardiographic assessment of the left ventricular (LV) structure and function was performed in anaesthetized adult WT and DKO mice (4 and 11 months old). It revealed an increase in LV internal diameter and volume during systole and diastole in DKO mice, without significant changes in the thickness of the ventricle walls (LV anterior wall, posterior wall, septum) (*Figure 2A and B*). Consistent with our observations, the calculated LV mass/body weight ratio was higher in DKO mice (*Figure 2C*). We found no differences in heart rate between DKO and WT mice (*Figure 2D*). Stroke volume and cardiac output were also significantly higher in the DKO than WT group (*Figure 2E and F*). The LV dilation observed in the DKO mice (increase in LV internal diameter and volume) significantly progressed over time (*Figure 2A and B*). Although the ejection fraction and fractional shortening were not significantly different between the WT and DKO groups at 4 months, they had significantly decreased in the DKO group by 11 months (*Figure 2G and H*). These observations suggest that DKO mice develop dilated cardiomyopathy with high output that progressively leads to heart failure. Consistent with these findings, plasma levels of atrial natriuretic peptide (ANP) and brain natriuretic peptide (BNP) were significantly higher in 5-month-old DKO mice than in single-KO and WT mice (*Figure 2I and J*). Measurement of the size of individual cardiomyocytes showed them to be significantly enlarged in the DKO mice (*Figure 2K and L*) but there were no obvious signs of cardiac fibrosis upon Picrosirius red staining at the age of five months (Supplementary material online, *Figure S5a* and *b*).

3.3 Combined loss of *Bmp*9 and *Bmp*10 leads to a reduction of arterial blood pressure, vascular abnormalities, and alveolar capillary dilatation

We next conducted experiments to identify the underlying mechanisms that could lead to the development of high-output heart failure (HOHF) in DKO mice. Because a fall in systemic arterial blood pressure (BP) is a feature of HOHF,[31] systemic arterial BP was first assessed in conscious mice using a non-invasive BP system (tail-cuff method, Kent Scientific Corporation). Systemic, diastolic, and mean BP were significantly lower in DKO than WT and single-KO mice (*Figure 3A–C*). We next determined whether the fall in systemic arterial BP was related to systemic arteriovenous shunting and/or peripheral vasodilatation. To detect systemic shunts, we injected 45-mm fluorescent microbeads into the systemic circulation via the left cardiac ventricle. The microbeads were efficiently trapped in the systemic vasculature in WT and single-KO mice, for example in the brain, but also readily crossed to the lungs in the DKO mice, leading to a massive accumulation of beads in the lungs (*Figure 3D*), supporting the presence of arteriovenous shunting or important dilations in the systemic vasculature. To detect pulmonary shunts, we intravenously injected 15-mm fluorescent microbeads. The fluorescent microbeads were efficiently trapped in the pulmonary arterioles and capillaries in WT and single-KO mice but not in 70% of DKO mice, in which the beads were able to reach other organs, such as the brain (*Figure 3E*), suggesting the presence of shunts or large dilations in the pulmonary vasculature. Using latex blue intra-ventricular injection, we observed that the latex progressed further in the vascular tree and small blood vessels in the intestines and brains of DKO than WT and single KO, mice suggesting dilated vessels in the DKO mice (*Figure 3F* and Supplementary material online, *Figure S6a* and *b*). Consistent with these observations, histological analysis of 500-nm thick lung sections revealed a two- to three-fold significant increase in the average size of the lung capillaries of DKO mice relative to that of WT mice (*Figure 3G and H*). In accordance with these results, the blood volume that could be collected from the DKO mice was significantly higher than that of the other groups (Supplementary material online, *Figure S6c*), perhaps partially explaining the observed splenomegaly and increased cardiac output.

Certain conditions, such as chronic anaemia and hyperthyroidism, can also be associated with elevated cardiac output. Thus, we measured haemoglobin levels (Supplementary material online, *Table S2*) and examined thyroid glands (Supplementary material online, *Figure S6d*), but no differences were noted.

Overall, our data show that the combined loss of *Bmp9* and *Bmp10* results in a decrease in peripheral vascular resistance in DKO mice, resulting in an increase in cardiac output, cardiomegaly, and the development of a HOHF phenotype with age.

3.4 RNAseq analysis reveals differential expression of genes involved in inflammation, angiogenesis, blood pressure, cilium organization and motility, and cardiac chamber development

We performed an RNAseq analysis of the lungs of WT and DKO mice to better understand what was happening in the DKO mice, specifically in the lungs, which are highly vascularized, and of specific interest in PH. Among the 17 853 identified genes, we observed 537 differentially expressed genes (DEGs) with adjusted *P*-values <0.05 and absolute log2 fold changes >log2 (1.5). The DEGs were distributed between 343 over-expressed and 194 under-expressed genes in DKO relative to WT mice. A bi-clustering heatmap designed to visualize the expression profile of the top 40 DEGs according to their statistical significance (lowest adjusted *P*-values) is presented in *Figure 4A*. We used DAVID tools to analyse the list of the 537 DEGs (Supplementary material online, *Figure S7* and *Table S3*), grouped the most relevant biological process gene ontology (GO) terms into six categories and highlighted the involved genes in volcano plots (*Figure 4B*, Supplementary material online, *Table S4*). We found 82 DEGs related to inflammation and the immune response, 38 to ion transport, 30 to extracellular matrix disassembly, 30 to cell adhesion, 18 to angiogenesis, and 14 to BP and vasoreactivity (*Figure 4B*, Supplementary material online, *Table S3*). Enriched molecular function GO terms confirmed these results (Supplementary material online, *Figure S7*). We also found several biological process GO terms linked to insulin secretion, haemostasis, cilium, iron ions, organ morphogenesis, and multicellular organism development (Supplementary material online, *Figure S7*). The Pi3K/AKT pathway, which has been shown to be activated when *Acvrl1* is deleted,[32] was enriched in both GO biological process and KEGG analyses (Supplementary material online, *Figure S7*). We performed gene set enrichment analysis (GSEA) on the full list of genes ranked by log2 fold change using the functional Gene Ontology/Biological Process database. The categories with the top positive

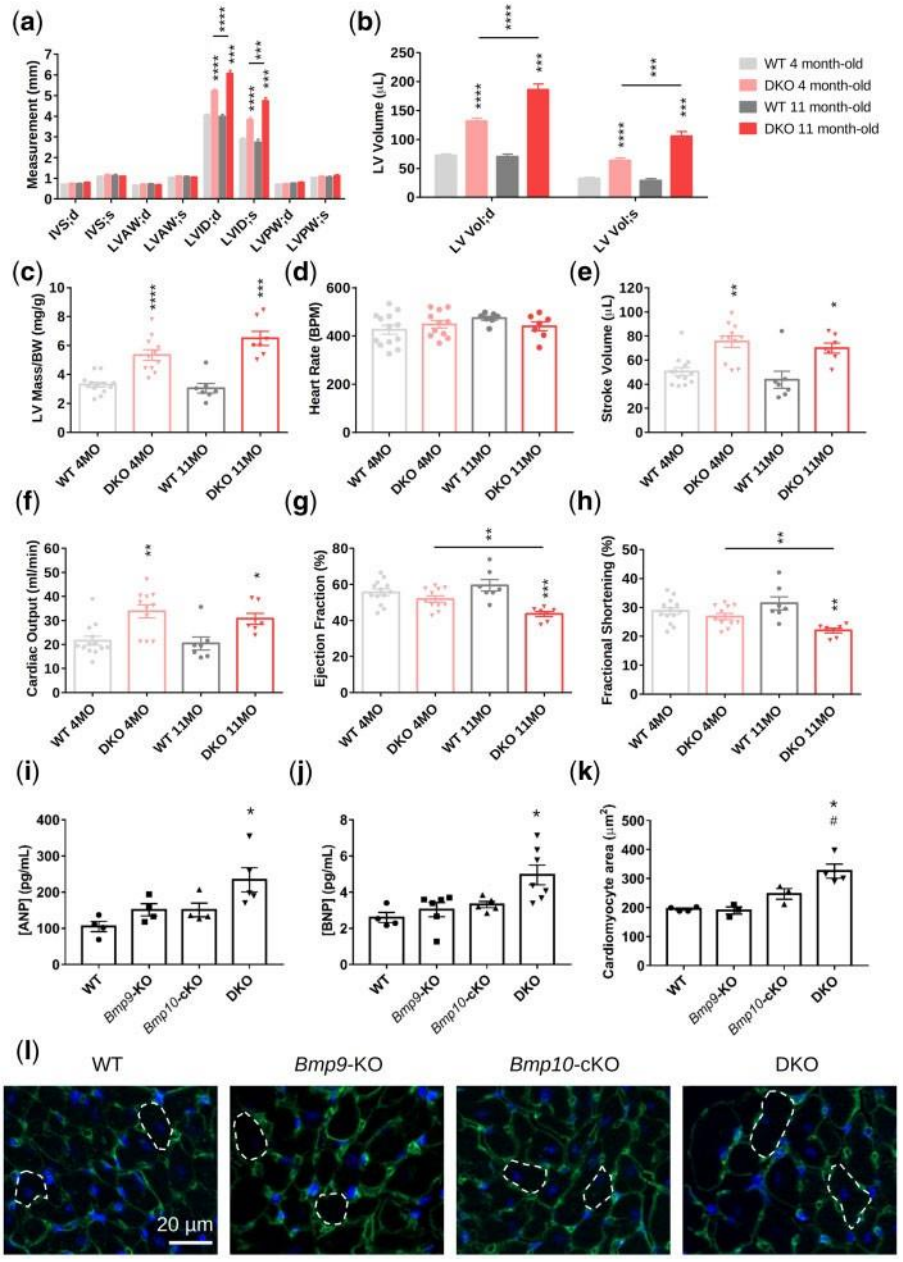

Figure 2 Combined loss of *Bmp9* and *Bmp10* leads to high cardiac output and cardiac hypertrophy in DKO mice. (*A*–*H*) Echocardiographic analysis of the left ventricle of 4- and 11-month-old WT and DKO female mice (n = 7–13/group). End-systolic (s) and end-diastolic (d) measurements of the interventricular septum (IV S), left ventricular anterior wall (LVAW), left ventricular posterior wall (LVPW) thickness, and the left ventricular internal diameter (LVID) (*A*), calculation of the left ventricular volume (LV Vol) (*B*), left ventricular mass/body weight (LV mass/BW) (*C*), heart rate (*D*), stroke volume (*E*), cardiac output (*F*), ejection fraction (*G*), and fractional shortening (*H*). All mice were injected with tamoxifen at the age of 2 months. Data are presented as the mean ± SEM and were analysed using Mann–Whitney tests to compare DKO vs. WT or 4-month-old vs. 11-month-old mice. *P < 0.05, **P < 0.01, ***P < 0.001, ****P < 0.0001. (*I*–*L*) Plasma analysis and immunofluorescence. ANP (atrial natriuretic peptide) (*I*) and BNP (brain natriuretic peptide) (*J*) plasma levels (n = 4–7 male mice/group). Quantitative analysis of cardiomyocyte size (*K*) and representative photomicrographs (*L*) of transverse heart sections stained with FITC-conjugated wheatgerm agglutinin to outline individual cardiomyocytes (n = 3–4 female mice/group, 100 cardiomyocytes/mouse). Mice were injected with tamoxifen at the age of 2 months and analysed at the age of 4–5 months. Data are presented as the means ± SEM and were analysed using Kruskal–Wallis tests followed by Dunn's tests. *P < 0.05 vs. WT; $^{\#}P$ < 0.05 vs. *Bmp9*-KO.

normalized enrichment score were related to inflammation (the first was the response to interleukin 1) and those with the top negative scores were linked to cilium organization and motility, cardiac chamber/ventricular system development, and response to BMP (*Figure 4C*). We next performed quantitative real-time reverse transcription polymerase chain reaction (RT-qPCR) of several DEGs or genes identified by the GSEA analysis using a different cohort of mice and studied their expression in both single and DKO mice (Supplementary material online, *Figure*

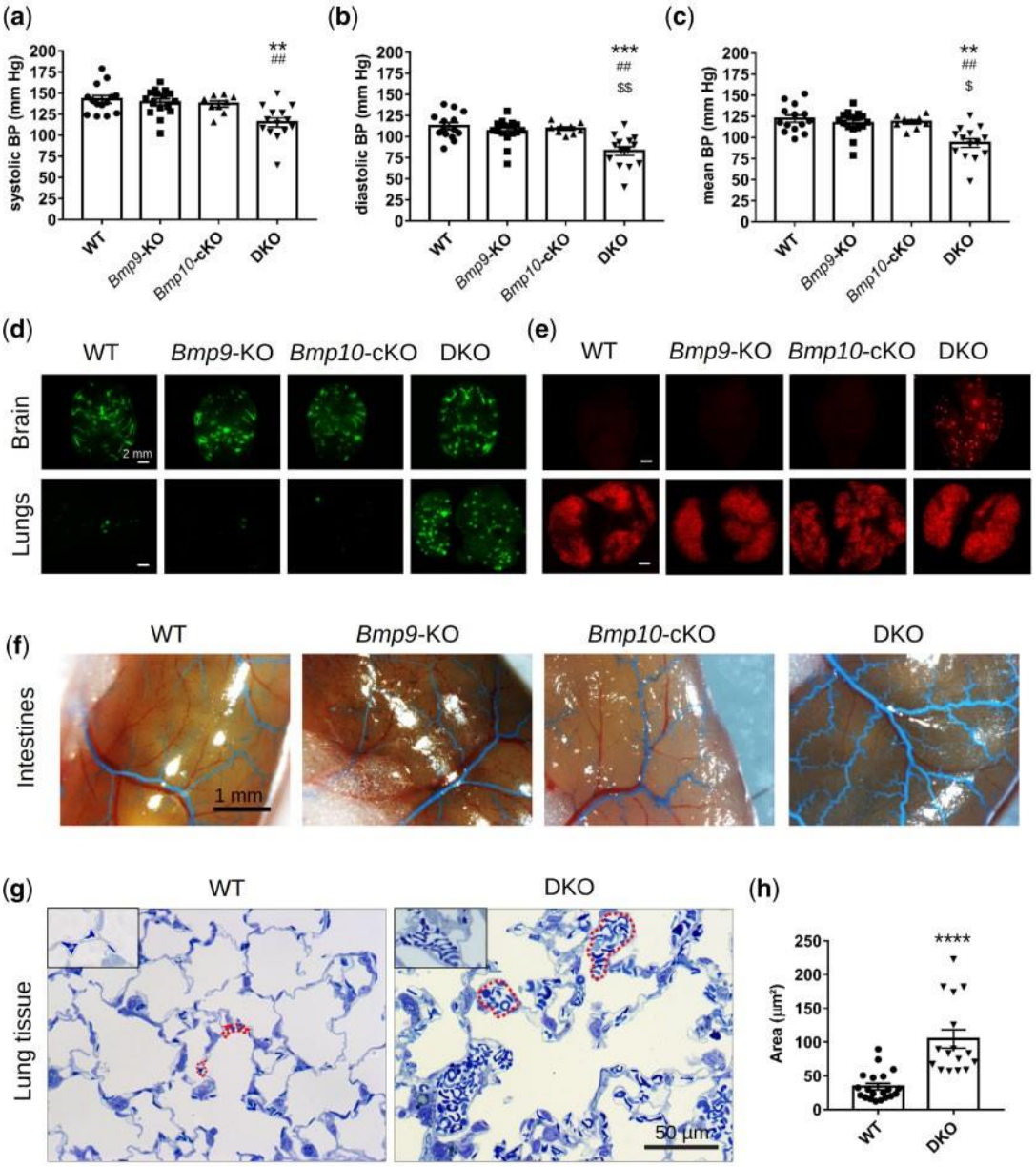

Figure 3 Combined loss of *Bmp9* and *Bmp10* leads to a reduction in arterial blood pressure (BP), vascular anomalies, and alveolar capillary dilatation in DKO mice. Non-invasive measurements of systolic (*A*), diastolic (*B*), and mean (*C*) BP in conscious adult mice (n = 9–16 male mice/group). Data are presented as the mean ± SEM and were analysed using Kruskal–Wallis tests followed by Dunn's tests. $^{**}P < 0.01$, $^{***}P < 0.001$ vs. WT. $^{\#\#}P < 0.01$ vs. *Bmp9*-KO. $^{\$}P < 0.05$, $^{\$\$}P < 0.01$ vs. *Bmp10*-cKO. Representative photomicrographs of brain and lungs of mice that received an injection of 45-mm fluorescent beads in the left cardiac ventricle (n = 5 female and 5 male mice/group, scale bar = 2 mm) (*D*) and of mice that received an intravenous injection of 15-mm fluorescent beads (n = 4 female and 3 male mice/group) (*E*). Representative photomicrographs of the intestines of latex-blue injected mice (*F*) (n = 3–5 male and 3–5 female mice/group, scale bar = 1 mm). Representative photomicrographs (*G*) and quantitative analysis (*H*) of the size of capillaries from 500-nm thick lung sections stained with epoxy tissue stain. The red dotted lines outline several capillaries (scale bar = 50 mm). Data represent the mean capillary area of n = 16–20 independent lung sections from three different female mice/group. Data are presented as the means ± SEM and were analysed using Mann–Whitney tests. $^{****}P < 0.0001$ vs. WT. Mice were injected with tamoxifen at the age of 2 months and analysed at the age of 5 months.

S8a and *b*). We confirmed elevated expression of two genes encoding key inflammatory mediators, *Ccl2* (encoding CCL2, also known as monocyte chemoattractant protein-1) and *Ccl3* (encoding CCL3, also known as macrophage inflammatory protein 1-alpha), but not *Cxcl5*. We also confirmed the reduced expression of two genes in the lungs of DKO mice involved in BP and vasoreactivity, *Smad6* and *Edn1* (encoding endothelin 1) (*Figures 4B and 7B*, Supplementary material online, *Figure S4a*). Consistent with these results, a reduction in endothelin-1 (ET-1) protein levels was also confirmed in the plasma of DKO mice (*Figure 7A*). We could not confirm the down-regulation of two genes involved in cilium

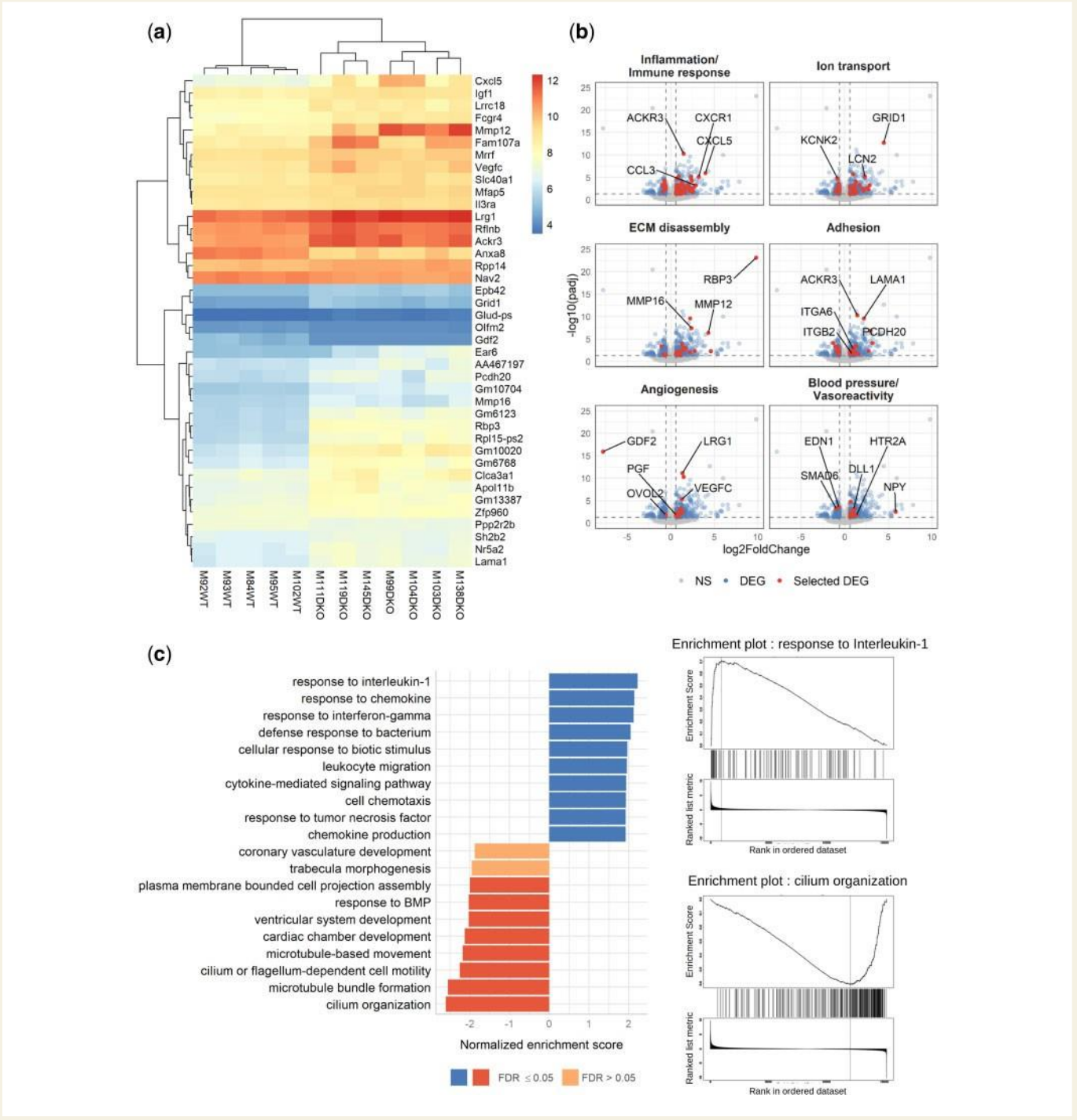

Figure 4 RNAseq analysis of WT and DKO mouse lung tissue reveals modulation of the transcription of genes involved in inflammation, angiogenesis, blood pressure, cilium organization, and cardiac development. Five WT and seven DKO male mice were injected with tamoxifen at the age of 2 months and analysed at the age of 5 months. (*A*) A bi-clustering heatmap was used to visualize the expression profile of the top 40 differentially expressed genes (DEGs) between the WT and DKO conditions, with the lowest adjusted *P*-value by plotting their log2 transformed expression values (colour scale) for each sample. (*B*) Visualization of the comparison of the global transcriptional change across groups was visualized by volcano plots. Each data point in the scatter plot represents a gene. The log2 fold change of each gene is represented on the *x*-axis and the -log10 of its adjusted *P*-value on the *y*-axis. Genes that were not significantly differentially expressed (NS) are represented in grey, DEGs in blue, and a selection of DEG involved in specific biological processes in red (gene ontologies used for these volcano plots are listed in the Supplementary material online, *Table S3*). (*C*) Gene-set enrichment analysis (GSEA) performed using the functional database gene ontology/biological process non-redundant. The top 10 positive (blue) and negative (red) categories are presented. Each bar represents a gene ontology, the normalized enrichment score is represented on the *x*-axis, and the colour of the bar represents the FDR *P*-value. Enrichment plots for the top positive and negative terms are shown on the right. .

motility, *Hydin* and *Dnah5* (data not shown). Surprisingly, our RNAseq analysis performed in the lungs highlighted the cardiac chamber development GO term. We thus performed an RT-qPCR analysis in heart tissue (left ventricle) from single KO and DKO mice of *Nkx2-5* (encoding the homeobox transcription factor Nkx2-5) and *Tbx-20* (encoding a T-box transcription factor Tbx20), two transcription factors that are important in cardiac development and known to be regulated by BMP10.[24,33] The mRNA levels of both transcription factors were reduced in the DKO mice, but only the decrease of Nkx2-5 reached statistical significance (Supplementary material online, *Figure S8b*). To further validate the inflammation/Immune response GO term, we next used the Cibersortx digital cytometry tool,[34] along with a mouse lung single-cell RNAseq dataset,[35] to estimate the relative abundance of various cell populations from our lung RNAseq analysis. Consistent with our histological observations (*Figure 1H*), we observed a significant increase in the estimated percentage of alveolar and interstitial macrophages in DKO versus WT mice (Supplementary material online, *Figure S8c* and *d*). We also observed an increase in the estimated percentage of vein cells, that may likely be a consequence of pulmonary vasodilation or possible venous congestion due to the development of HOHF in this DKO mouse model (*Figure 3G*, Supplementary material online, *Figure S8c* and *d*). Consistent with our GSEA results, which highlighted the cilium organization GO term, the estimated percentage of ciliated cells was reduced (*Figure 4C*, Supplementary material online, *Figure S8c* and *d*). Overall, these results show that there is strong inflammation in the lungs of the DKO mice and that genes that are crucial for cardiovascular homeostasis are deregulated in the absence of *Bmp9* and *Bmp10*.

3.5 Hypoxia-induced pulmonary vascular and cardiac remodelling in *Bmp9*-KO, *Bmp10*-cKO, and DKO mice

Chronic hypoxia induces adaptive pulmonary arterial muscularization and right ventricular hypertrophy[26,36] and we previously showed that *Bmp9*-KO mice are partially protected from such remodelling.[26] Thus, we next determined and compared the susceptibility of *Bmp9*-KO, *Bmp10*-cKO, and DKO mice to develop PH in response to chronic hypoxia (10% FiO_2) for 3 weeks (*Figures 5 and 6*).

We confirmed that *Bmp9*-KO mice do not develop spontaneous PH under normoxic conditions and that they are mildly protected against PH induced by chronic hypoxia, as reflected by a significant decrease in the values of the right ventricular systolic pressure (RVSP) and Fulton index [RV/(LVþS)], indicators of right ventricular hypertrophy (*Figure 5A and B*), and the percentage of medial wall thickness and muscularized distal pulmonary arteries (*Figure 6A*).

Under normoxic conditions, *Bmp10*-cKO mice did not develop spontaneous PH. There were no significant differences in the RVSP values, percentage of medial wall thickness or muscularized distal pulmonary arteries, or Fulton index [RV/(LVþS)] between *Bmp10*-cKO and WT mice (*Figures 5D and E, 6B*). After 3 weeks of exposure to hypoxia, we observed a similar increase in RVSP values, Fulton index, and the percentage of medial wall thickness and muscularized distal pulmonary arteries of the *Bmp10*-cKO mice relative to the those of the WT mice (*Figures 5D and E, 6B*). Interestingly, the heart weight of *Bmp10*-cKO mice exposed to chronic hypoxia was greater than that of hypoxic WT mice and those maintained in normoxia (*Figure 5F*). Of note, there was no significant increase in heart weight of *Bmp9*-KO mice when challenged with chronic hypoxia (*Figure 5C*).

Under normoxic conditions, the DKO mice did not develop spontaneous PH, similarly to the *Bmp9*-KO and *Bmp10*-cKO mice (*Figures 5G and H, 6C*). However, they exhibited HOHF, as reflected by a marked increase in the Fulton index [RV/(LVþS)] and heart weight (*Figure 5H and I*). DKO mice chronically exposed to hypoxia exhibited an attenuated increase in RVSP values and the percentage of medial wall thickness and muscularized distal pulmonary arteries relative to hypoxic WT mice (*Figures 5G and 6C*).

Overall, these results show that *Bmp10* deletion does not offer protection from PH, whereas *Bmp9* deletion or double *Bmp9/Bmp10* deletion can partially protect against the pulmonary vascular remodelling induced by chronic hypoxia.

3.6 BMP9 is an endothelin-1-mediated vasoconstrictor

ET-1 is a potent vasoconstrictor peptide that contributes to the pulmonary vascular remodelling associated with PH. Consistent with our previous work and publications showing that BMP9 can affect ET-1 expression,[26] we found significantly lower circulating ET-1 protein levels in the plasma of *Bmp9*-KO and DKO mice than in that of WT mice, but not in *Bmp10*-cKO mice (*Figure 7A*). This result is consistent with the RNAseq analysis showing the differential expression of genes involved in vasoreactivity, including *Edn1* (*Figure 4B*, Supplementary material online, *Table S3*). Lung ET-1 mRNA levels were also significantly lower in DKO than WT mice but not in *Bmp10*-cKO mice (*Figure 7B*). Consistent with this notion, we previously showed that BMP9 is a potent vasoconstrictor using the chicken embryo chorioallantoic membrane (CAM) assay.[19] To better characterize the important regulators of vascular tone regulated by BMP9, we tested three different inhibitors of vasoconstriction, namely bosentan (endothelin receptor antagonist), captopril (angiotensin-converting enzyme inhibitor), and terguride (serotonin receptor antagonist) in the CAM assay in response to BMP9. Vessels were visualized by injecting fluorescein-labelled dextran (FITC-dextran) into the CAM vessels. In accordance with our previous work,[19] BMP9 induced the vasoconstriction of the blood vessels in the treated area, interrupting the passage of FITC-dextran in these vessels (*Figure 7C and D*). BMP9-induced vasoconstriction was inhibited by Bosentan (at the 500-mM dose) (*Figure 7C and D*) but not captopril or terguride (Supplementary material online, *Figure S9*). These data support that ET-1 is a key component of BMP9-induced vasoconstriction.

4. Discussion

The first link between PAH and germline mutations in *BMPR2* was established 20 years ago. Since then, several mutations in this pathway have been added to the list of genes involved in PAH (e.g. *ACVRL1, ENG*, and *SMAD9*) and, more recently, mutations in the genes *BMP9* (also called *GDF2*) and *BMP10,* encoding the two high-affinity ligands for ALK1/BMPRII.[3–8] It was thus hypothesized that the loss of these ligands could be an essential driver of disease pathogenesis. This was underscored by the demonstration that the administration of recombinant BMP9 can attenuate the development of PH in animal models.[27] However, in 2019, in contrast to what was expected, we found that blocking BMP9 had beneficial effects and prevented the muscularization of pulmonary arteries in PH animal models.[26] Interestingly, defects in this pathway have also been associated with vascular abnormalities, such as excessive capillary fusion (AVM), hyperdilation, reduced vascular muscularization, and excessive/abnormal angiogenesis and vessel patterning.[23,37,38] However, the

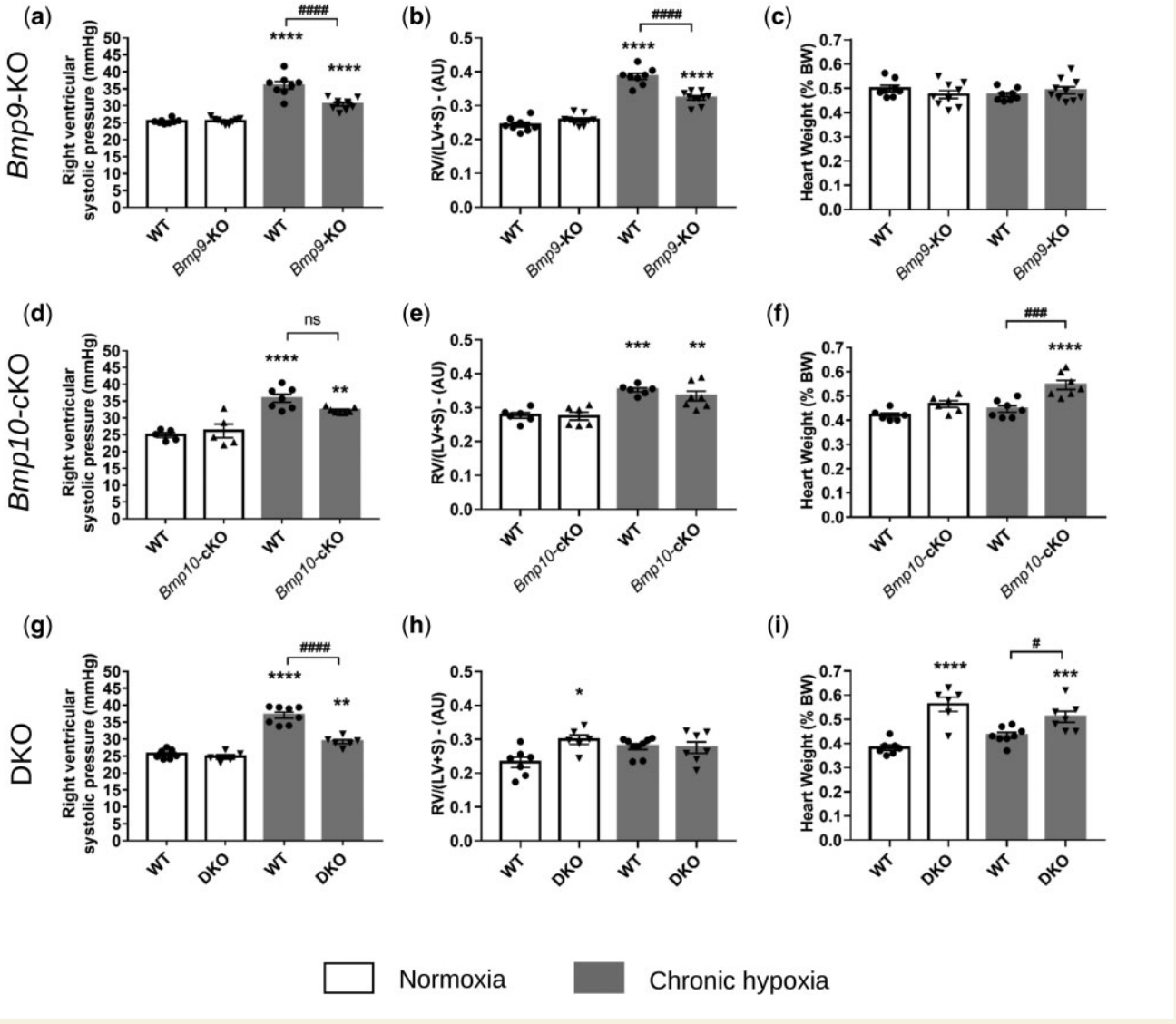

Figure 5 *Bmp9*-KO, *Bmp10*-cKO, and DKO mice do not develop spontaneous PH under normoxic conditions and exhibit different susceptibility to the development of chronic hypoxia induced PH and cardiac remodelling. (*A, D, G*) Values of right ventricular systolic pressure (RVSP), (*B, E, H*) right ventricular hypertrophy, expressed by the Fulton Index RV/(LVþS), (*C, F, I*), and of heart weight of WT vs. *Bmp9*-KO mice (*A–C*), WT vs. *BMP10*-cKO mice (*D–F*), and WT vs. DKO mice (*G–I*). Data are presented as the means ± SEM of n = 5–10 male mice per group and were analysed using by ANOVA followed by Tukey's test. *$P < 0.05$, **$P < 0.01$, ***$P < 0.001$, ****$P < 0.0001$ vs. WT under normoxia; $^{\#}P < 0.05$, $^{\#\#\#}P < 0.001$, $^{\#\#\#\#}P < 0.0001$ vs. WT under chronic hypoxia. AU, arbitrary unit; LV, left ventricle; ns, non-significant; RV, right ventricle; S, septum.

phenotypes of adult mice lacking *Bmp9* and/or *Bmp10* have never been thoroughly described and compared. The aim of the present study was to address, for the first time, the roles of BMP9 and BMP10 in pulmonary and cardiovascular homeostasis, more specifically, in the context of PAH, using adult single and double knockout mice under normoxic and hypoxic conditions (to induce PH). The deletion of *Bmp9* was constitutive and that of *Bmp10* induced at the adult stage to bypass embryonic lethality. We found that none of these transgenic mice developed spontaneous PH under unstressed conditions. *Bmp9* and *Bmp10* single knockout homozygous mutant adult mice were viable and fertile and exhibited no overt phenotype. However, deletion of *Bmp*10 in *Bmp*9-KO mice (DKO mice) led to several abnormalities of the cardiovascular and pulmonary systems (reduced BP, cardiomegaly, pulmonary inflammation and hemosiderosis). Furthermore, although the loss of *Bmp10* had no impact on the degree of pulmonary vascular remodelling induced by chronic hypoxia, *Bmp9*-KO and DKO mice chronically exposed to hypoxia exhibited less pronounced remodelling of the pulmonary vascular bed than their WT littermates. On the other hand, the loss of *Bmp10* under chronic hypoxia induced cardiomegaly. Overall, our data indicate both redundant and specific roles for BMP9 and BMP10 in vascular remodelling.

Under physiological conditions, the loss of one of the ligands (BMP9 or BMP10) did not lead to overt cardiovascular defects in adult C57Bl/6 mice, suggesting that one can compensate for the loss of the other. However, the combined loss of *Bmp*9 and *Bmp*10 had dramatic consequences on pulmonary and cardiovascular homeostasis and led to the

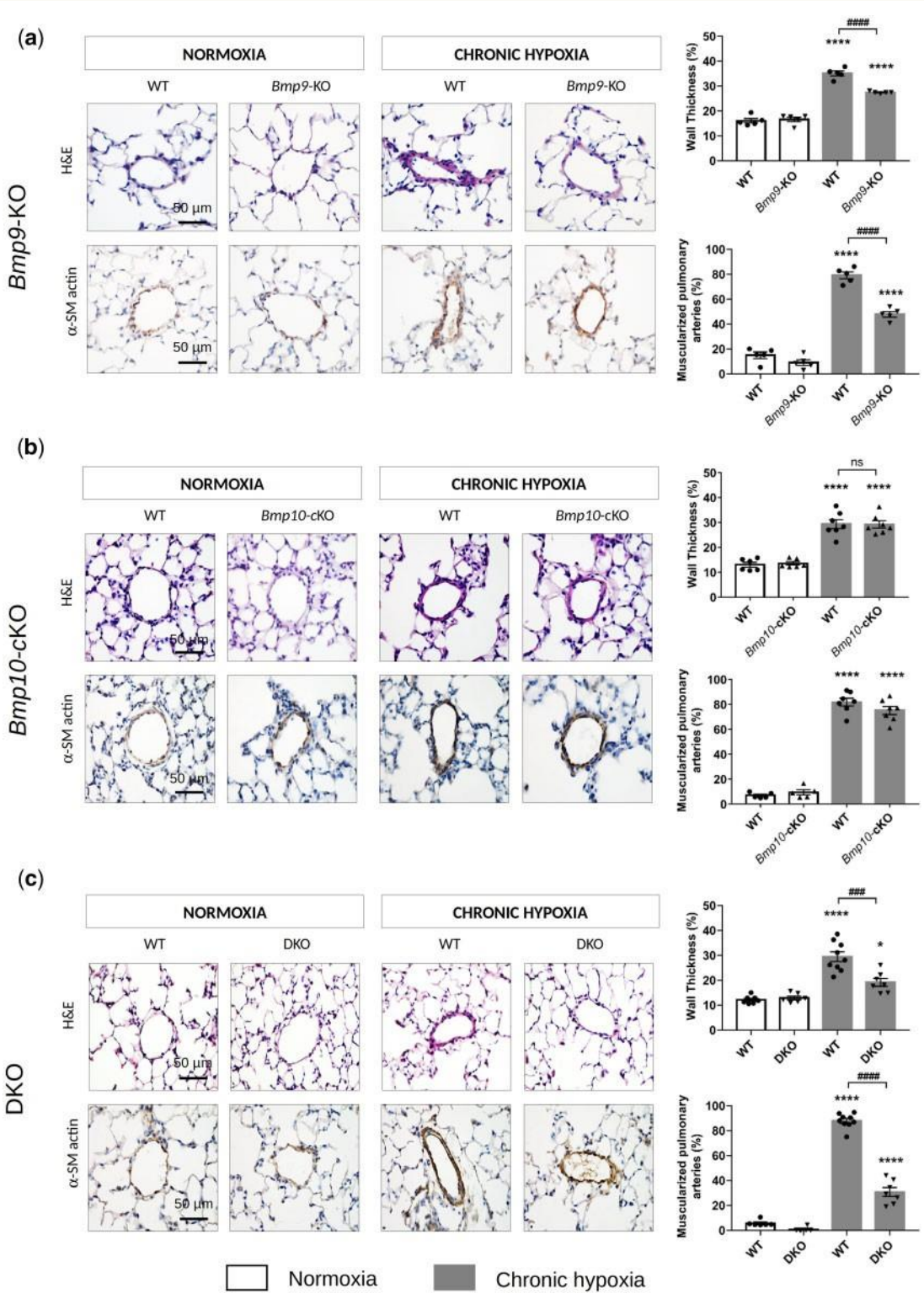

Figure 6 Loss of *Bmp9* but not *Bmp10* decreases the susceptibility of developing of chronic hypoxia-induced PH, as it protects against pulmonary arterial remodelling. Representative images of haematoxylin-eosin (H&E) staining and a-smooth muscle (SM)-actin and quantification of the percentage of muscularized and wall thickness of distal pulmonary arteries in the lungs of WT vs. *Bmp9*-KO mice (*A*), WT vs. *Bmp10*-cKO mice (*B*), and WT vs. DKO mice (*C*). Scale bar = 50 mm for all sections. Data are presented as the means ± SEM of $n = 5–9$ male mice per group and were analysed by ANOVA followed by Tukey's test. *$P < 0.05$, ****$P < 0.0001$ vs. WT under normoxia; $^{\#\#\#}P < 0.001$, $^{\#\#\#\#}P < 0.0001$ vs. WT under chronic hypoxia.

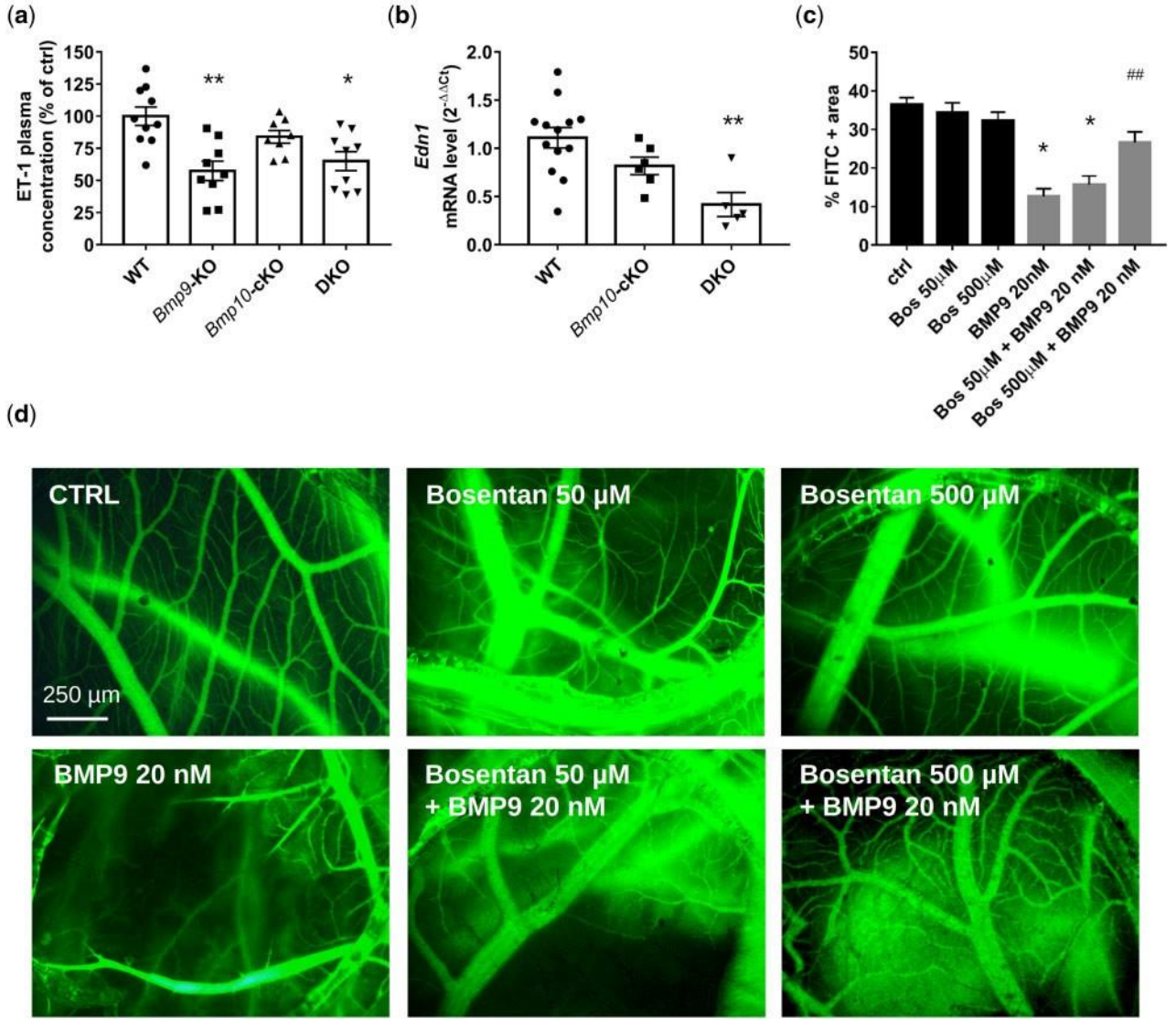

Figure 7 Loss of *Bmp9* in mice is associated with reduced endothelin-1 (ET-1) abundance and ET-1 plays a crucial role in BMP9-induced vasoconstriction in chick chorioallantoic membrane. ET-1 plasma (*A*) levels in WT, *Bmp9*-KO, *Bmp10*-cKO, and DKO mice (n = 8–10 male mice/group) and lung mRNA (*B*) in WT, *Bmp10*-cKO, and DKO mice (n = 5–13 male mice/group). Mice were injected with tamoxifen at the age of 2 months and analysed at the age of 5 months. Data are presented as the mean ± SEM and were analysed using Kruskal–Wallis tests followed by Dunn's tests. *P < 0.05, **P < 0.01 vs. WT. Quantitative analysis (*C*) and representative photomicrographs (*D*) of FITC-Dextran-injected blood vessels from chick chorioallantoic membranes treated with bosentan (0, 50, and 500 mM), in combination with BMP9 (20 nM) or not for 24 h (scale bar = 250 um). Data are presented as the means ± SEM of n = 3–6 eggs/group and were analysed using Kruskal–Wallis tests followed by Dunn's tests. *P < 0.05 vs. vehicle treated control and $^{\#\#}P$ < 0.01 vs. the 20 nM BMP9 condition.

progressive development of HOHF, with cardiomegaly and increased cardiomyocyte size and ANP and BNP levels. We show that systemic BP is reduced in DKO mice, which is a sign of a reduced peripheral vascular resistance that can cause HOHF. This can arise from vasodilation and/or arteriovenous shunting. Indeed, we observed that blood vessels were dilated, especially in the lungs, intestines, and brain, which is intriguing, as the BMP9/BMP10 receptor ALK1 is predominantly expressed by endothelial cells in these organs (EC Atlas[39]) We also observed the abnormal passage of fluorescent microbeads from pulmonary arteries to pulmonary veins and from systemic arteries to systemic veins in DKO mice. Our results are in accordance with those of a recent study be Wang *et al.*,[40] published while our manuscript was under revision, showing vasodilatation, a decrease in peripheral arterial wall thickness, and lower systemic BP in a different mouse model with a double deletion of *Bmp*9 and *Bmp*10. Interestingly, the loss of endothelial *Eng* in adult mice also leads to HOHF and AVMs, but the underlying mechanism appears to be different. Indeed, the authors show an exaggerated endothelial response to VEGF signalling, favouring the formation of AVMs in the pelvic area,[41] whereas, in our study, the vascular dilations or shunts were not limited to one specific location. Our results are also different from those obtained from the loss of *Acvrl1* in adult mice, which is associated with pulmonary and gastrointestinal haemorrhage, severe anaemia, and the

development of HOHF, ultimately leading to death within three weeks.[42,43] Here, DKO mice survived for several months after tamoxifen administration. This could either be due to differences in the efficiency of tamoxifen-induced deletion, genetic differences, or to BMP9/10-independent ALK1 functions. These DKO mice share certain features with HHT and could be a valuable mouse model in the field of vascular anomalies, allowing long-term studies on adult mice.

The marked hemosiderosis (presence of iron-laden macrophages) and inflammation observed in DKO lungs could have been caused by heart failure (leading to venous congestion and alveolar bleeding) or compromised endothelial integrity or pulmonary circulation or could have resulted from a direct effect on inflammation. Consistent with these results, RNA-seq analysis showed that the main up-regulated functions were linked to inflammation (key inflammatory chemokines, such as CCL2 and CCL3, were confirmed by RTqPCR to be up-regulated in the DKO mice), with an increased estimated percentage of alveolar and interstitial macrophages in the DKO mice, supporting that BMP9 and BMP10 likely play important roles in inflammation. The relationship between this pathway and inflammation is also supported by recent publications suggesting that BMP9 and BMP10 can prevent macrophage recruitment, in part, via the inhibition of CCL2.[44] Blood vessel-related functions (angiogenesis, regulation of BP) were also significantly deregulated in the RNAseq analysis and these results are in accordance with the observed phenotype (vasodilation, reduced systemic BP) and the down-regulation of ET-1 in the plasma.

In addition to the alteration in peripheral vascular resistance contributing to the development of HOHF in the DKO mice, we cannot exclude direct effects of the combined loss of BMP9 and BMP10 on the heart. BMP10 is known to be predominantly expressed in the heart, where it plays a central role in cardiomyogenesis in prenatal and postnatal life.[20,24] However, it has also been implicated in the maintenance of vascular development, homeostasis, and remodelling.[20,23,25,45,46] Consistent with such roles, we found reduced expression of the gene encoding the cardiogenic transcription factor NKX2-5 in the heart of the DKO mice. Although it is currently well accepted that BMP9 could potentially compensate for the loss of *Bmp10* at the vascular level, to a certain degree, this does not appear to be the case for the cardiomyogenic program.[20,23,25] *Bmp10*-KO mice indeed die between E9.5 and E10.5, with profound defects in cardiac development[24]; the receptor and signalling molecules involved are yet to be determined. BMP10 binds with high affinity to ALK1, of which the expression is restricted to endothelial cells, but which has also been shown to bind in a complex with ALK3, which is expressed by cardiomyocytes and a subset of endothelial cells of the heart (EC Atlas[39]) Here, we provide the first *in vivo* demonstration that the loss of *Bmp10* in adult C57Bl/6 mice does not have any overt phenotypic defects in cardiac tissue or function under unstressed conditions. However, these mice developed marked cardiac enlargement when chronically exposed to hypoxia, supporting that BMP10 plays a crucial role in cardiac remodelling in adulthood. Consistent with our present findings, it was previously shown that disruption of the downstream effector Smad4 in cardiomyocytes leads to cardiac hypertrophy and heart failure.[47]

We previously showed that mice lacking *Bmp9* do not develop spontaneous PH and that its inhibition attenuates chronic hypoxia-induced pulmonary vascular remodelling.[26] Here, we confirm these results in the *Bmp9*-KO and DKO mice and additionally show that the loss of *Bmp10* has no impact on the percentage of medial wall thickness and muscularized distal pulmonary arteries. These results suggest a specific role of BMP9 in this context. Similarly, we have previously shown that BMP9, but not BMP10, plays a role in tumour angiogenesis using the same knockout mouse models.[29] This may be due to a difference between BMP9 and BMP10 in terms of their affinity for BMP receptors, quantity, availability, or the activity of ligands or receptor complexes in a given organ and in response to hypoxia. Interestingly, we found a significant reduction in pSmad1/5/8 and pSmad2/3 protein levels in lung tissues from mice lacking *Bmp9* (i.e. *Bmp9*-KO and DKO mice), but not those lacking *Bmp10*. Consistent with these results, ET-1 levels were reduced in mice lacking *Bmp9*, but not mice lacking *Bmp10*, supporting previous results obtained by our group and others showing that the BMP9 pathway is involved in lung vascular tone through the modulation of central vasoactive factors.[5,26,48,49] RNA-seq analysis also showed modulation of the expression of genes involved in vasoreactivity, including *Edn1*. We previously reported that BMP9 can induce vasoconstriction in the CAM. Here, we confirmed and extended this notion by showing that such BMP9-induced vasoconstriction is abolished in the presence of bosentan, a dual endothelin receptor antagonist. These results reinforce the hypothesis of altered vasoconstriction in *Bmp9*-KO lung vessels, which could protect the mice from the development of PH and are consistent with the current therapeutic strategies that rely on vasodilators, such as bosentan.

Our data obtained in *Bmp9*-KO mice may appear to be at odds with human genetic data and have been extensively discussed,[50–52] but were confirmed here in the DKO mice. It should be kept in a mind that a limitation of mouse studies is that they develop mild PH with no plexiform lesions. Therefore it would be informative to confirm these findings in rat models of severe PH. BMPs signal through several heterocomplexes composed of type I and type II receptors, which can be modulated by accessory receptors and endogenous ligand traps. BMP signalling is thus complex and context-dependent and the low penetrance of most of the mutations that affect the BMPR-II pathway must be considered.[53] The recent discovery of *BMP9* and *BMP10* mutations in PAH patients further supports the involvement of this signalling pathway in the development of PAH, but the underlying mechanisms in humans are still unknown. Certain *BMP9* mutations have recently been associated with impaired processing and secretion and reduced activity in plasma, whereas others have no functional consequences.[54] Biochemical characterization for *BMP10* mutations has not been yet reported, but given the importance of *BMP10* in heart morphogenesis, these mutations could cause primary cardiac problems that increase the risk of developing PH. Indeed, one of the rare patients with a *BMP10* mutation presented with features of congenital heart disease.[55] Moreover, the relationship between BMP9 and BMP10 plasma levels and the risk of developing PAH is not clear and is yet to be clearly demonstrated.

Twenty years after the discovery of *BMPR2* mutations, there are still no clinically approved treatments for PAH that target BMP signalling. Our data suggest that although blocking BMP9 could be beneficial in PH, blocking BMP10 may have no effect on pulmonary vascular remodelling and could have detrimental effects on cardiac remodelling, and blocking both BMP9 and BMP10 over a long period of time might have adverse effects, such as excessive vasodilation, HOHF, and lung inflammation. Although we previously showed protective effects of the BMP9/BMP10 ligand trap ALK-1 ECD in rat models, this treatment was only administered for 2 weeks.[26] In accordance with our results, it was recently shown that long-term treatment with BMP9 induced aberrant endothelial to mesenchymal transition in PAH pulmonary endothelial cells due to exacerbated pro-inflammatory signalling[56] Overall, these observations warrant caution for therapeutic strategies targeting this pathway in terms of specificity, dose, and length of treatment.

In conclusion, our data suggest redundant roles for BMP9 and BMP10 in cardiovascular homeostasis under normoxic conditions (as only the combined loss of both *Bmp9* and *Bmp10* led to reduced vascular resistance, reduced BP, cardiomegaly, and development of the HOHF phenotype) but also highlight specific roles under chronic hypoxic conditions. We obtained evidence that BMP9 contributes to chronic hypoxia-induced pulmonary vascular remodelling, whereas BMP10 plays a role in hypoxia-induced cardiac remodelling in mice.

Supplementary material

Supplementary material is available at *Cardiovascular Research* online.

Authors' contributions

Conception or design: C.B., L.T., C.G., and S.B.; drafting of the manuscript: C.B., C.G., and S.B.; conducted experiments and/or performed data analysis: all. All authors reviewed and revised the final version and approved submission of the manuscript.

Acknowledgements

The authors thank Raphaël Thuillet, Mina Ottaviani, Mustapha Chelgham, Antoine Wawrzyniak, the CEA-Grenoble medical biology lab, and Matthieu Rolland for technical assistance and advice. The authors also thank Helen Arthur for sharing the protocol for arteriovenous shunt detection using fluorescent beads and Hervé Pointu, Soumalamaya Bama, Irène Jeannin, and Charlène Magallon for their help in the maintenance of our mouse colonies.

Conflict of interest: Over the last three years, C.G. reports grants from Acceleron and Janssen and grants and personal fees from Merck, outside the submitted work. M.H. and L.S. report grants, personal fees, and non-financial support from Actelion, Bayer, GlaxoSmithKline, and MSD outside of the submitted work. M.H. is a member of the Scientific Advisory Board of Morphogen-IX. All other authors have no conflicts of interest to disclose.

Funding

This research was supported by grants from the French National Agency for Research (ANR), ANR-17-CE14-0006 (B9inPH) and ANR-15-IDEX-02 (IDEX-IRS2018 ANGIOBMP), and in part by the CEA (Commissariat a` l'Energie Atomique et aux Energies Alternatives, DRF/IRIG/DS), the National Institute for Health and Medical Research (INSERM), the University of Grenoble and the University of Paris-Saclay, the Association Maladie de Rendu-Osler (AMRO/HHT-France), the Fondation pour la Recherche Médicale (EQU202003010188), and the H2020-msca-ITN-2018 (V.A.Cure-814316). The authors acknowledge the animal facility platform supported by GRAL, a programme of the Chemistry Biology Health (CBH) Graduate School of University Grenoble Alpes (ANR-17-EURE-0003). This work was partially performed by a laboratory member of the France Life Imaging network (grant ANR-11-INBS-0006). N.B. is a recipient of a PhD fellowship from the Ile-de-France region (ARDoc Health).

Data availability

Datasets are available in the online supplement and have been deposited on the arrayexpress website https://www.ebi.ac.uk/arrayexpress/experiments/E-MTAB-10392/, last accessed date : June 7th 2021.

References

1. Simonneau G, Montani D, Celermajer DS, Denton CP, Gatzoulis MA, Krowka M, Williams PG, Souza R. Haemodynamic definitions and updated clinical classification of pulmonary hypertension. *Eur Respir J* 2019;53:1801913.
2. Humbert M, Guignabert C, Bonnet S, Dorfmuller P, Klinger JR, Nicolls MR, Olschewski AJ, Pullamsetti SS, Schermuly RT, Stenmark KR, Rabinovitch M. Pathology and pathobiology of pulmonary hypertension: state of the art and research perspectives. *Eur Respir J* 2019;53:1801887.
3. Evans JD, Girerd B, Montani D, Wang XJ, Galie N, Austin ED, Elliott G, Asano K, Grunig E, Yan Y, Jing ZC, Manes A, Palazzini M, Wheeler LA, Nakayama I, Satoh T, Eichstaedt C, Hinderhofer K, Wolf M, Rosenzweig EB, Chung WK, Soubrier F, Simonneau G, Sitbon O, Graf S, Kaptoge S, Di Angelantonio E, Humbert M, Morrell NW. BMPR2 mutations and survival in pulmonary arterial hypertension: an individual participant data meta-analysis. *Lancet Respir Med* 2016;4:129–137.
4. Morrell NW, Aldred MA, Chung WK, Elliott CG, Nichols WC, Soubrier F, Trembath RC, Loyd JE. Genetics and genomics of pulmonary arterial hypertension. *Eur Respir J* 2019;53:1801899.
5. David L, Mallet C, Mazerbourg S, Feige JJ, Bailly S. Identification of BMP9 and BMP10 as functional activators of the orphan activin receptor-like kinase 1 (ALK1) in endothelial cells. *Blood* 2007;109:1953–1961.
6. Rhodes CJ, Batai K, Bleda M, Haimel M, Southgate L, Germain M, Pauciulo MW, Hadinnapola C, Aman J, Girerd B, Arora A, Knight J, Hanscombe KB, Karnes JH, Kaakinen M, Gall H, Ulrich A, Harbaum L, Cebola I, Ferrer J, Lutz K, Swietlik EM, Ahmad F, Amouyel P, Archer SL, Argula R, Austin ED, Badesch D, Bakshi S, Barnett C, Benza R, Bhatt N, Bogaard HJ, Burger CD, Chakinala M, Church C, Coghlan JG, Condliffe R, Corris PA, Danesino C, Debette S, Elliott CG, Elwing J, Eyries M, Fortin T, Franke A, Frantz RP, Frost A, Garcia JGN, Ghio S, Ghofrani HA, Gibbs JSR, Harley J, He H, Hill NS, Hirsch R, Houweling AC, Howard LS, Ivy D, Kiely DG, Klinger J, Kovacs G, Lahm T, Laudes M, Machado RD, MacKenzie Ross RV, Marsolo K, Martin LJ, Moledina S, Montani D, Nathan SD, Newnham M, Olschewski A, Olschewski H, Oudiz RJ, Ouwehand WH, Peacock AJ, Pepke-Zaba J, Rehman Z, Robbins I, Roden DM, Rosenzweig EB, Saydain G, Scelsi L, Schilz R, Seeger W, Shaffer CM, Simms RW, Simon M, Sitbon O, Suntharalingam J, Tang H, Tchourbanov AY, Thenappan T, Torres F, Toshner MR, Treacy CM, Vonk Noordegraaf A, Waisfisz Q, Walsworth AK, Walter RE, Wharton J, White RJ, Wilt J, Wort SJ, Yung D, Lawrie A, Humbert M, Soubrier F, Tregouet DA, Prokopenko I, Kittles R, Graf S, Nichols WC, Trembath RC, Desai AA, Morrell NW, Wilkins MR; UK NIHR BioResource Rare Diseases Consortium; UK PAH Cohort Study Consortium; US PAH Biobank Consortium. Genetic determinants of risk in pulmonary arterial hypertension: international genome-wide association studies and meta-analysis. *Lancet Respir Med* 2019;7:227–238.
7. Wang G, Fan R, Ji R, Zou W, Penny DJ, Varghese NP, Fan Y. Novel homozygous BMP9 nonsense mutation causes pulmonary arterial hypertension: a case report. *BMC Pulm Med* 2016;16:17.
8. Wang XJ, Lian TY, Jiang X, Liu SF, Li SQ, Jiang R, Wu WH, Ye J, Cheng CY, Du Y, Xu XQ, Wu Y, Peng FH, Sun K, Mao YM, Yu H, Liang C, Shyy JY, Zhang SY, Zhang X, Jing ZC. Germline BMP9 mutation causes idiopathic pulmonary arterial hypertension. *Eur Respir J* 2019;53:1801609.
9. Graf S, Haimel M, Bleda M, Hadinnapola C, Southgate L, Li W, Hodgson J, Liu B, Salmon RM, Southwood M, Machado RD, Martin JM, Treacy CM, Yates K, Daugherty LC, Shamardina O, Whitehorn D, Holden S, Aldred M, Bogaard HJ, Church C, Coghlan G, Condliffe R, Corris PA, Danesino C, Eyries M, Gall H, Ghio S, Ghofrani HA, Gibbs JSR, Girerd B, Houweling AC, Howard L, Humbert M, Kiely DG, Kovacs G, MacKenzie Ross RV, Moledina S, Montani D, Newnham M, Olschewski A, Olschewski H, Peacock AJ, Pepke-Zaba J, Prokopenko I, Rhodes CJ, Scelsi L, Seeger W, Soubrier F, Stein DF, Suntharalingam J, Swietlik EM, Toshner MR, van Heel DA, Vonk Noordegraaf A, Waisfisz Q, Wharton J, Wort SJ, Ouwehand WH, Soranzo N, Lawrie A, Upton PD, Wilkins MR, Trembath RC, Morrell NW. Identification of rare sequence variation underlying heritable pulmonary arterial hypertension. *Nat Commun* 2018;9:1416.
10. Johnson DW, Berg JN, Baldwin MA, Gallione CJ, Marondel I, Yoon SJ, Stenzel TT, Speer M, Pericak-Vance MA, Diamond A, Guttmacher AE, Jackson CE, Attisano L, Kucherlapati R, Porteous ME, Marchuk DA. Mutations in the activin receptor-like kinase 1 gene in hereditary haemorrhagic telangiectasia type 2. *Nat Genet* 1996;13:189–195.
11. McAllister KA, Grogg KM, Johnson DW, Gallione CJ, Baldwin MA, Jackson CE, Helmbold EA, Markel DS, McKinnon WC, Murrell J. Endoglin, a TGF-beta binding protein of endothelial cells, is the gene for hereditary haemorrhagic telangiectasia type 1. *Nat Genet* 1994;8:345–351.

12. Wooderchak-Donahue WL, McDonald J, O'Fallon B, Upton PD, Li W, Roman BL, Young S, Plant P, Fülöp GT, Langa C, Morrell NW, Botella LM, Bernabeu C, Stevenson DA, Runo JR, Bayrak-Toydemir P. BMP9 mutations cause a vascular-anomaly syndrome with phenotypic overlap with hereditary hemorrhagic telangiectasia. *Am J Hum Genet* 2013;93:530–537.
13. Tillet E, Bailly S. Emerging roles of BMP9 and BMP10 in hereditary hemorrhagic telangiectasia. *Front Genet* 2014;5:456.
14. Breitkopf-Heinlein K, Meyer C, König C, Gaitantzi H, Addante A, Thomas M, Wiercinska E, Cai C, Li Q, Wan F, Hellerbrand C, Valous NA, Hahnel M, Ehlting C, Bode JG, Müller-Bohl S, Klingmüller U, Altenöder J, Ilkavets I, Goumans M-J, Hawinkels LJAC, Lee S-J, Wieland M, Mogler C, Ebert MP, Herrera B, Augustin H, Sánchez A, Dooley S, Ten Dijke P. BMP-9 interferes with liver regeneration and promotes liver fibrosis. *Gut* 2017;66:939–954.
15. Tillet E, Ouarne M, Desroches-Castan A, Mallet C, Subileau M, Didier R, Lioutsko A, Belthier G, Feige JJ, Bailly S. A heterodimer formed by bone morphogenetic protein 9 (BMP9) and BMP10 provides most BMP biological activity in plasma. *J Biol Chem* 2018;293:10963–10974.
16. Neuhaus H, Rosen V, Thies RS. Heart specific expression of mouse BMP-10 a novel member of the TGF-beta superfamily. *Mech Dev* 1999;80:181–184.
17. Susan-Resiga D, Essalmani R, Hamelin J, Asselin MC, Benjannet S, Chamberland A, Day R, Szumska D, Constam D, Bhattacharya S, Prat A, Seidah NG. Furin is the major processing enzyme of the cardiac-specific growth factor bone morphogenetic protein 10. *J Biol Chem* 2011;286:22785–22794.
18. Jiang H, Salmon RM, Upton PD, Wei Z, Lawera A, Davenport AP, Morrell NW, Li W. The prodomain-bound form of bone morphogenetic protein 10 is biologically active on endothelial cells. *J Biol Chem* 2016;291:2954–2966.
19. David L, Mallet C, Keramidas M, Lamande N, Gasc JM, Dupuis-Girod S, Plauchu H, Feige JJ, Bailly S. Bone morphogenetic protein-9 is a circulating vascular quiescence factor. *Circ Res* 2008;102:914–922.
20. Chen H, Brady Ridgway J, Sai T, Lai J, Warming S, Chen H, Roose-Girma M, Zhang G, Shou W, Yan M. Context-dependent signaling defines roles of BMP9 and BMP10 in embryonic and postnatal development. *Proc Natl Acad Sci USA* 2013;110:11887–11892.
21. Townson SA, Martinez-Hackert E, Greppi C, Lowden P, Sako D, Liu J, Ucran JA, Liharska K, Underwood KW, Seehra J, Kumar R, Grinberg AV. Specificity and structure of a high affinity activin receptor-like kinase 1 (ALK1) signaling complex. *J Biol Chem* 2012;287:27313–27325.
22. Salmon RM, Guo J, Wood JH, Tong Z, Beech JS, Lawera A, Yu M, Grainger DJ, Reckless J, Morrell NW, Li W. Molecular basis of ALK1-mediated signalling by BMP9/BMP10 and their prodomain-bound forms. *Nat Commun* 2020;11:1621.
23. Ricard N, Ciais D, Levet S, Subileau M, Mallet C, Zimmers TA, Lee SJ, Bidart M, Feige JJ, Bailly S. BMP9 and BMP10 are critical for postnatal retinal vascular remodeling. *Blood* 2012;119:6162–6171.
24. Chen H, Shi S, Acosta L, Li W, Lu J, Bao S, Chen Z, Yang Z, Schneider MD, Chien KR, Conway SJ, Yoder MC, Haneline LS, Franco D, Shou W. BMP10 is essential for maintaining cardiac growth during murine cardiogenesis. *Development* 2004;131:2219–2231.
25. Levet S, Ouarne M, Ciais D, Coutton C, Subileau M, Mallet C, Ricard N, Bidart M, Debillon T, Faravelli F, Rooryck C, Feige JJ, Tillet E, Bailly S. BMP9 and BMP10 are necessary for proper closure of the ductus arteriosus. *Proc Natl Acad Sci USA* 2015;112:E3207–E3215.
26. Tu L, Desroches-Castan A, Mallet C, Guyon L, Cumont A, Phan C, Robert F, Thuillet R, Bordenave J, Sekine A, Huertas A, Ritvos O, Savale L, Feige J-J, Humbert M, Bailly S, Guignabert C. Selective BMP-9 inhibition partially protects against experimental pulmonary hypertension. *Circ Res* 2019;124:846–855.
27. Long L, Ormiston ML, Yang X, Southwood M, Graf S, Machado RD, Mueller M, Kinzel B, Yung LM, Wilkinson JM, Moore SD, Drake KM, Aldred MA, Yu PB, Upton PD, Morrell NW. Selective enhancement of endothelial BMPR-II with BMP9 reverses pulmonary arterial hypertension. *Nat Med* 2015;21:777–785.
28. Nikolic I, Yung LM, Yang P, Malhotra R, Paskin-Flerlage SD, Dinter T, Bocobo GA, Tumelty KE, Faugno AJ, Troncone L, McNeil ME, Huang X, Coser KR, Lai CSC, Upton PD, Goumans MJ, Zamanian RT, Elliott CG, Lee A, Zheng W, Berasi SP, Huard C, Morrell NW, Chung RT, Channick RW, Roberts KE, Yu PB. Bone morphogenetic protein 9 is a mechanistic biomarker of portopulmonary hypertension. *Am J Respir Crit Care Med* 2019;199:891–902.
29. Ouarne M, Bouvard C, Boneva G, Mallet C, Ribeiro J, Desroches-Castan A, Soleilhac E, Tillet E, Peyruchaud O, Bailly S. BMP9, but not BMP10, acts as a quiescence factor on tumor growth, vessel normalization and metastasis in a mouse model of breast cancer. *J Exp Clin Cancer Res* 2018;37:209.
30. Desroches-Castan A, Tillet E, Ricard N, Ouarne M, Mallet C, Belmudes L, Coute Y, Boillot O, Scoazec JY, Bailly S, Feige JJ. Bone morphogenetic protein 9 is a paracrine factor controlling liver sinusoidal endothelial cell fenestration and protecting against hepatic fibrosis. *Hepatology* 2019;70:1392–1408.
31. Mehta PA, Dubrey SW. High output heart failure. *QJM* 2009;102:235–241.
32. Ola R, Dubrac A, Han J, Zhang F, Fang JS, Larrivee B, Lee M, Urarte AA, Kraehling JR, Genet G, Hirschi KK, Sessa WC, Canals FV, Graupera M, Yan M, Young LH, Oh PS, Eichmann A. PI3 kinase inhibition improves vascular malformations in mouse models of hereditary haemorrhagic telangiectasia. *Nat Commun* 2016;7:13650.
33. Sun L, Yu J, Qi S, Hao Y, Liu Y, Li Z. Bone morphogenetic protein-10 induces cardiomyocyte proliferation and improves cardiac function after myocardial infarction. *J Cell Biochem* 2014;115:1868–1876.
34. Newman AM, Steen CB, Liu CL, Gentles AJ, Chaudhuri AA, Scherer F, Khodadoust MS, Esfahani MS, Luca BA, Steiner D, Diehn M, Alizadeh AA. Determining cell type abundance and expression from bulk tissues with digital cytometry. *Nat Biotechnol* 2019;37:773–782.
35. Travaglini KJ, Nabhan AN, Penland L, Sinha R, Gillich A, Sit RV, Chang S, Conley SD, Mori Y, Seita J, Berry GJ, Shrager JB, Metzger RJ, Kuo CS, Neff N, Weissman IL, Quake SR, Krasnow MA. A molecular cell atlas of the human lung from single-cell RNA sequencing. *Nature* 2020;587:619–625.
36. Tamura Y, Phan C, Tu L, Le Hiress M, Thuillet R, Jutant EM, Fadel E, Savale L, Huertas A, Humbert M, Guignabert C. Ectopic upregulation of membrane-bound IL6R drives vascular remodeling in pulmonary arterial hypertension. *J Clin Invest* 2018;128:1956–1970.
37. Garcia de Vinuesa A, Abdelilah-Seyfried S, Knaus P, Zwijsen A, Bailly S. BMP signaling in vascular biology and dysfunction. *Cytokine Growth Factor Rev* 2016;27:65–79.
38. Oh SP, Seki T, Goss KA, Imamura T, Yi Y, Donahoe PK, Li L, Miyazono K, ten Dijke P, Kim S, Li E. Activin receptor-like kinase 1 modulates transforming growth factor-beta 1 signaling in the regulation of angiogenesis. *Proc Natl Acad Sci USA* 2000;97:2626–2631.
39. Kalucka J, de Rooij L, Goveia J, Rohlenova K, Dumas SJ, Meta E, Conchinha NV, Taverna F, Teuwen LA, Veys K, Garcia-Caballero M, Khan S, Geldhof V, Sokol L, Chen R, Treps L, Borri M, de Zeeuw P, Dubois C, Karakach TK, Falkenberg KD, Parys M, Yin X, Vinckier S, Du Y, Fenton RA, Schoonjans L, Dewerchin M, Eelen G, Thienpont B, Lin L, Bolund L, Li X, Luo Y, Carmeliet P. Single-cell transcriptome atlas of murine endothelial cells. *Cell* 2020;180:764–779 e720.
40. Wang L, Rice M, Swist S, Kubin T, Wu F, Wang S, Kraut S, Weissmann N, Bottger T, Wheeler M, Schneider A, Braun T. BMP9 and BMP10 act directly on vascular smooth muscle cells for generation and maintenance of the contractile state. *Circulation* 2021;143:1394–1410.
41. Tual-Chalot S, Garcia-Collado M, Redgrave RE, Singh E, Davison B, Park C, Lin H, Luli S, Jin Y, Wang Y, Lawrie A, Jakobsson L, Arthur HM. Loss of endothelial endoglin promotes high-output heart failure through peripheral arteriovenous shunting driven by VEGF signaling. *Circ Res* 2020;126:243–257.
42. Park SO, Wankhede M, Lee YJ, Choi EJ, Fliess N, Choe SW, Oh SH, Walter G, Raizada MK, Sorg BS, Oh SP. Real-time imaging of de novo arteriovenous malformation in a mouse model of hereditary hemorrhagic telangiectasia. *J Clin Invest* 2009;119:3487–3496.
43. Morine KJ, Qiao X, Paruchuri V, Aronovitz MJ, Mackey EE, Buiten L, Levine J, Ughreja K, Nepali P, Blanton RM, Karas RH, Oh SP, Kapur NK. Conditional knockout of activin like kinase-1 (ALK-1) leads to heart failure without maladaptive remodeling. *Heart Vessels* 2017;32:628–636.
44. Upton PD, Park JES, De Souza PM, Davies RJ, Griffiths MJD, Wort SJ, Morrell NW. Endothelial protective factors BMP9 and BMP10 inhibit CCL2 release by human vascular endothelial cells. *J Cell Sci* 2020;133:jcs239715.
45. Capasso TL, Li B, Volek HJ, Khalid W, Rochon ER, Anbalagan A, Herdman C, Yost HJ, Villanueva FS, Kim K, Roman BL. BMP10-mediated ALK1 signaling is continuously required for vascular development and maintenance. *Angiogenesis* 2020;23:203–220.
46. Laux DW, Young S, Donovan JP, Mansfield CJ, Upton PD, Roman BL. Circulating Bmp10 acts through endothelial Alk1 to mediate flow-dependent arterial quiescence. *Development* 2013;140:3403–3412.
47. Wang J, Xu N, Feng X, Hou N, Zhang J, Cheng X, Chen Y, Zhang Y, Yang X. Targeted disruption of Smad4 in cardiomyocytes results in cardiac hypertrophy and heart failure. *Circ Res* 2005;97:821–828.
48. Star GP, Giovinazzo M, Langleben D. Bone morphogenic protein-9 stimulates endothelin-1 release from human pulmonary microvascular endothelial cells: a potential mechanism for elevated ET-1 levels in pulmonary arterial hypertension. *Microvasc Res* 2010;80:349–354.
49. Park JE, Shao D, Upton PD, Desouza P, Adcock IM, Davies RJ, Morrell NW, Griffiths MJ, Wort SJ. BMP-9 induced endothelial cell tubule formation and inhibition of migration involves Smad1 driven endothelin-1 production. *PLoS One* 2012;7:e30075.
50. Morrell NW, Upton PD, Li W, Yu PB. Letter by Morrell et al. regarding article, "Selective BMP-9 inhibition partially protects against experimental pulmonary hypertension". *Circ Res* 2019;124:e81.
51. Guignabert C, Tu L, Feige JJ, Humbert M, Bailly S. Response by Guignabert et al. to letter regarding article, "Selective BMP-9 inhibition partially protects against experimental pulmonary hypertension". *Circ Res* 2019;124:e82–e83.
52. Ormiston ML, Godoy RS, Chaudhary KR, Stewart DJ. The janus faces of bone morphogenetic protein 9 in pulmonary arterial hypertension. *Circ Res* 2019;124:822–824.
53. Larkin EK, Newman JH, Austin ED, Hemnes AR, Wheeler L, Robbins IM, West JD, Phillips JA 3rd, Hamid R, Loyd JE. Longitudinal analysis casts doubt on the presence of genetic anticipation in heritable pulmonary arterial hypertension. *Am J Respir Crit Care Med* 2012;186:892–896.

54. Hodgson J, Swietlik EM, Salmon RM, Hadinnapola C, Nikolic I, Wharton J, Guo J, Liley J, Haimel M, Bleda M, Southgate L, Machado RD, Martin JM, Treacy CM, Yates K, Daugherty LC, Shamardina O, Whitehorn D, Holden S, Bogaard HJ, Church C, Coghlan G, Condliffe R, Corris PA, Danesino C, Eyries M, Gall H, Ghio S, Ghofrani H-A, Gibbs JSR, Girerd B, Houweling AC, Howard L, Humbert M, Kiely DG, Kovacs G, Lawrie A, MacKenzie Ross RV, Moledina S, Montani D, Olschewski A, Olschewski H, Ouwehand WH, Peacock AJ, Pepke-Zaba J, Prokopenko I, Rhodes CJ, Scelsi L, Seeger W, Soubrier F, Suntharalingam J, Toshner MR, Trembath RC, Vonk Noordegraaf A, Wort SJ, Wilkins MR, Yu PB, Li W, Gräf S, Upton PD, Morrell NW. Characterization of GDF2 mutations and levels of BMP9 and BMP10 in pulmonary arterial hypertension. *Am J Respir Crit Care Med* 2020;201:575–585.

55. Eyries M, Montani D, Nadaud S, Girerd B, Levy M, Bourdin A, Tresorier R, Chaouat A, Cottin V, Sanfiorenzo C, Prevot G, Reynaud-Gaubert M, Dromer C, Houeijeh A, Nguyen K, Coulet F, Bonnet D, Humbert M, Soubrier F. Widening the landscape of heritable pulmonary hypertension mutations in paediatric and adult cases. *Eur RespirJ* 2019;53:1801371.

56. Szulcek R, Sanchez-Duffhues G, Rol N, Pan X, Tsonaka R, Dickhoff C, Yung LM, Manz XD, Kurakula K, Kiełbasa SM, Mei H, Timens W, Yu PB, Bogaard H-J, Goumans M-J. Exacerbated inflammatory signaling underlies aberrant response to BMP9 in pulmonary arterial hypertension lung endothelial cells. *Angiogenesis* 2020;23:699–714.

Translational perspective

Twenty years after the discovery of *BMPR2* mutations, there are still no clinically approved treatments for pulmonary arterial hypertension (PAH) that target BMP signalling. Our data suggest, using *Bmp9* and *Bmp10* single and double-knockout mice, that although blocking BMP9 could be beneficial in pulmonary hypertension, blocking BMP10 may have no effect on pulmonary vascular remodelling and could have detrimental effects on cardiac remodelling. Overall, these observations warrant caution for therapeutic strategies targeting this pathway and support that further studies are needed to understand how this complex pathway is involved in maintaining cardiovascular homeostasis in health and contributes to PAH and hereditary haemorrhagic telangiectasia (HHT).